

THREE-DIMENSIONAL MIXED MODE FRACTURE OF CEMENT MORTAR

K. Zhong, K. W. Lo and T. Tamilselvan

National University of Singapore, 10 Kent Ridge Crescent, Singapore 119260

ABSTRACT

In practice, most engineering components undergo complex three-dimensional loading and contain, or are assumed to contain, cracks or crack-like flaws. However, theoretical and experimental studies on mixed mode I, II and III fracture have only just begun in recent years.

In this study, a generalised criterion for the extension of a mixed mode fracture surface in three dimensions is proposed as an extension of the *unified model*, based on the notion of a simple conversion of pure mode to mixed mode loading energy, in direct proportion to their respective fracture energies. The criterion may be represented as the 3-dimensional surface depicted in Figure 1.

The proposed criterion has been tested against the behaviour of beam specimens (Figure 2) of cement mortar which were subjected to three- or four-point bending, as well as four-point shear. A grooved ligament which was rotated both vertically and horizontally with respect to the beam section was formed in the specimen, where each specimen had different orientations of the ligament and were subject to various loading combinations, so as to provide mixed mode loading conditions at the crack front. In doing so, the crack might be initiated and hence guided to extend along the truncated V-shaped throat segment as a mixed mode fracture, thereby providing a means of verifying the efficacy of the fracture envelope. The stress intensity factors K_I , K_{II} and K_{III} , of the respective modes of deformation were determined by three-dimensional finite element analysis, where the data pre-processing was undertaken by PATRAN, while the solution process was carried out by ABAQUS. The results of the analyses, as well as measurements made on the INSTRON 1334 servo-hydraulic testing machine, will be presented in the following text, and the proposed fracture criterion thereby validated.

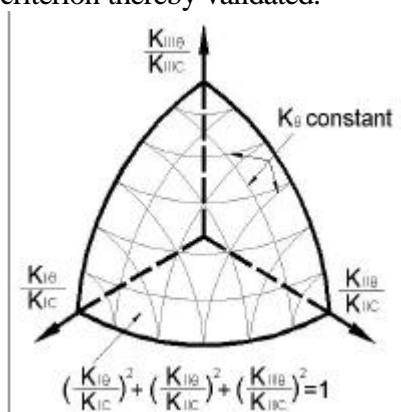


Figure 1: Unified mixed mode I, II and III fracture envelope

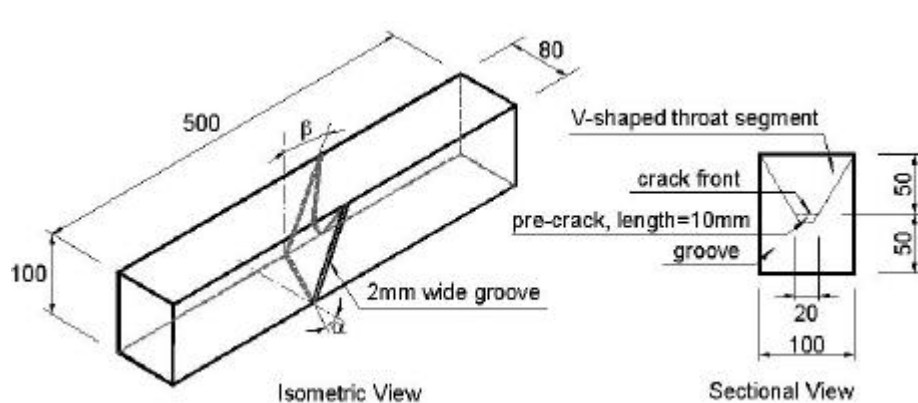


Figure 2: Beam specimen subject to mixed mode I, II and III loading (units in mm)

THREE-DIMENSIONAL MIXED MODE FRACTURE OF CEMENT MORTAR

K. Zhong, K. W. Lo and T. Tamilselvan

National University of Singapore, 10 Kent Ridge Crescent, Singapore 119260

ABSTRACT

A generalised criterion for the extension of a mixed mode fracture surface in three dimensions is proposed. The criterion has been tested against the behaviour of beam specimens of cement mortar which were subjected to three- and four-point bending, as well as four-point shear. A grooved ligament which was rotated vertically as well as horizontally with respect to the beam section was formed in the specimen, where each specimen had different orientations of the ligament, so as to provide differing mixed mode loading conditions at the crack front. In doing so, the crack could be initiated and hence guided to extend along the truncated V-shaped throat segment as a mixed mode fracture, thereby providing a means of verifying the efficacy of the fracture envelope.

The stress intensity factors K_I , K_{II} and K_{III} , of the respective modes of deformation were determined by finite element analysis, where the data pre-processing was undertaken by PATRAN, while the solution process was carried out by ABAQUS. As a result of the analyses, as well as measurements made on the INSTRON 1334 servo-hydraulic testing machine, the proposed fracture envelope was confirmed.

KEYWORDS

Three-dimensional fracture testing, mixed mode fracture criterion, cement mortar specimens, FE analysis.

INTRODUCTION

In practice, most structural components undergo mixed mode loading involving tension as well as in- and out-of-plane shearing. Studies on mixed modes I, II and III fracture have been the subject of research in recent decades. Various fracture criteria have been proposed, among which the maximum tangential stress criterion proposed by Erdogan and Sih [1] and the minimum strain energy criterion proposed by Sih [2] are the more commonly used in the study of mixed mode crack growth. The application of these criteria has been extended to mixed modes I, II and III loading [3]. However, it has been reported that none of the criteria give satisfactory results under all loading conditions [4].

On the other hand, Richard and Kuna [5] have developed a loading device to achieve mixed modes I, II and III, as well as respective pure mode fractures on plexiglass and aluminium specimens, while Hyde and Aksogan [6] have used an axisymmetric bar-type specimen containing conical “crack-like” external flaws to obtain mixed modes I, II and III fracture data. Apart from the foregoing reports, laboratory tests on mixed modes I, II and III fracture are rarely found in the corresponding literature, and this may be due to the complexities of specimen geometries and loading conditions that are involved in such applications.

In the following discussion, a mixed mode I, II and III fracture criterion and test method to verify the criterion, which is based on cement mortar beam specimens, will be proposed. The stress intensity factors of the respective modes of loading have been evaluated numerically from three-dimensional finite element analysis. The results of the analyses and measurements from corresponding laboratory tests will be presented subsequently, and shown to confirm the validity of the proposed fracture criterion.

BACKGROUND OF THEORY

Similarly as in the case of the *unified model* [7], for pure mode III loading, the energy release rate $G_{III\theta}$ along the generalized plane of Figure 1 may be expressed via closure analysis as

$$G_{III\theta} = \frac{1}{\delta a} \int_0^{\delta a} [\hat{\sigma}_{\theta z}(r, \theta) \cdot u'_{zz}(\delta a - r, \pi)] dr, \quad (1)$$

where the $\hat{\sigma}_{\theta z}(r, \theta)$ is the shear stress along the generalized plane, $u_{zz}(a-r, \theta)$ the displacement of the crack edge along the z direction, as referred to the kinked branch tip, and a the length of the kinked branch crack. Next, by adopting $K_{III\theta}$ as the unified mode III stress intensity factor with respect to the generalized plane, it may be shown that

$$K_{III\theta} = \lim_{r \rightarrow 0} \tau_{\theta z} \sqrt{2\pi r} = K_{III} \left(\cos \frac{\theta}{2} \cos \theta + \sin \frac{\theta}{2} \sin \theta \right), \quad (2)$$

where K_{III} is the mode III stress intensity factor along the self-similar direction, defined as

$$K_{III} = \lim_{r \rightarrow 0} \tau_{\theta z}(r, 0) \sqrt{2\pi r}. \quad (3)$$

Since the stress intensity factor K_{III} , which is referred to the generalised direction of the kinked branch tip, may be specified as

$$K'_{III} = \lim_{(r-\delta a) \rightarrow 0} \tau'_{\theta z}(r-\delta a, 0) \sqrt{2\pi(r-\delta a)}, \quad (4)$$

in the limiting condition in which $a \rightarrow 0$ and K_{III} would thereby have to be evaluated with respect to the main crack tip, $K_{III} = K_{III\theta}$. Hence, Eqn. 2 may be simplified as

$$G_{III\theta} = (1 + \nu) \frac{K_{III\theta}^2}{E} \quad (5)$$

(a more detailed derivation may be obtained from reference [8]).

As a result of invoking the principle of superposition, the overall rate of energy release, G_θ , due to crack extension in the generalized plane when subjected to mixed mode I, II and III loading, may be determined as

$$G_\theta = G_{I\theta} + G_{II\theta} + G_{III\theta}, \quad (6)$$

where $G_{I\theta}$ and $G_{II\theta}$ are the energy release rates for the tensile and shearing modes of deformation respectively. Therefore, in the state of fracture,

$$G_\theta = G_C, \quad (7)$$

where G_C would be the generalized mixed mode critical rate of energy release. Next, based on a pro-rata energy conversion rate of

$$G_{I\alpha} + G_{II\alpha} + G_{III\alpha} = G_{I\alpha} \frac{G_C}{G_{IC}} + G_{II\alpha} \frac{G_C}{G_{IIC}} + G_{III\alpha} \frac{G_C}{G_{IIIC}}, \quad (8)$$

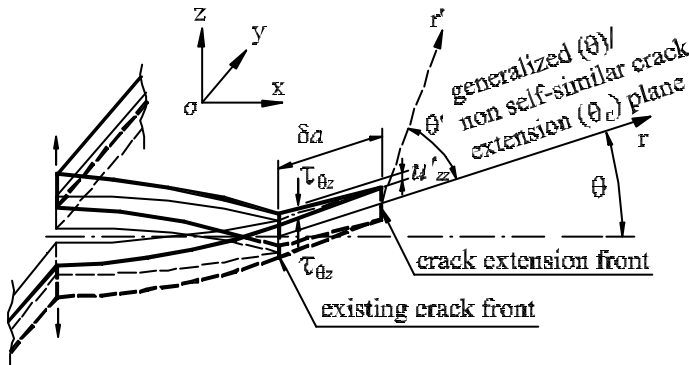
in view of Eqn. 6 and 7, the generalised mixed mode I, II and III fracture criterion may be expressed as

$$\frac{G_{I\alpha}}{G_{IC}} + \frac{G_{II\alpha}}{G_{IIC}} + \frac{G_{III\alpha}}{G_{IIIC}} = 1, \quad (9)$$

or alternatively re-stated as

$$\frac{K_{I\alpha}}{K_{IC}} + \frac{K_{II\alpha}}{K_{IIC}} + \frac{K_{III\alpha}}{K_{IIIC}} = 1, \quad (10)$$

as depicted by the envelope of Figure 2.



Note: notation referred to crack extension tip is primed; e.g. $r' = r - \delta a$ when $\theta' = 0$

Figure 1: Closure parameters for mode III crack extension

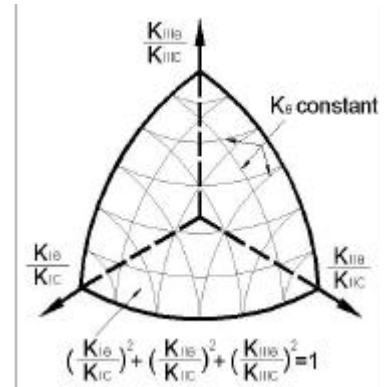


Figure 2: Unified mixed mode I, II and III fracture envelope

LABORATORY TESTING AND FINITE ELEMENT ANALYSIS

Experimental Materials

Ordinary Portland Cement and natural, fine-graded sand were used to cast the mortar specimens. The mix proportions of cement : water : sand by weight was 1.0 : 0.31 : 0.8. The materials were mixed in a drum mixer for a period of not less than 10 minutes to ensure its uniformity. The mean compressive cube strength was measured as 86MPa in tests carried out according to BS 1881: Part 116 [9]. Stainless steel moulds were used for the specimens which were cured in the fog room for 28 days.

Geometry of Specimen

Figure 3 illustrates the design of the beam specimen. The overall dimensions of the specimen was 500mm (length) 100mm (depth) 80mm (width). In order to have a mixed mode I-II-III fracture, a 2mm wide grooved ligament, which was rotated both vertically (angle θ_v) and horizontally (angle θ_h) was formed in the specimen, leaving a V-shaped throat segment. This was done by fixing a thin, stainless steel shim, coated with mould oil, to the mould before casting, and then removing it within 3 hours of casting so as not to adhere to the specimen. The ligament was located such that the mid-crack-front coincided with the centre of the specimen. Two values were chosen for θ_v and θ_h , namely 26.56 and 45 respectively. Hence, four groups of beam configuration with differing combinations of θ_v and θ_h values were available for testing.

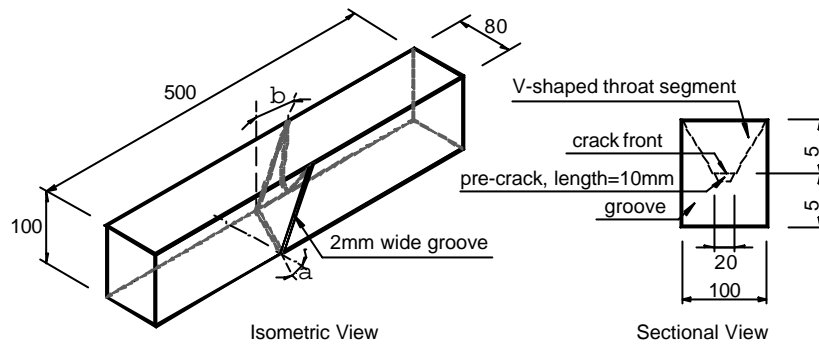


Figure 3: Geometry of beam specimen (units in mm)

Laboratory Set-up and Testing Procedures

The tests were conducted on the INSTRON 1334 servo-hydraulic testing machine. In order to achieve different mode I/mode II and mode I/mode III loading ratios, each beam group was subjected to three loading cases, as depicted in Figure 4. In all cases, the specimen was simply-supported.

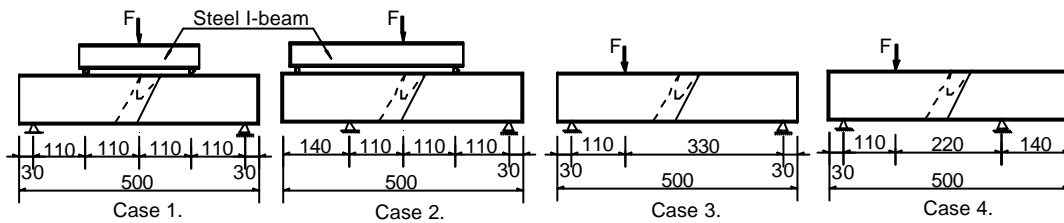


Figure 4: Loading cases used in tests

The load was then applied monotonically at a rate of 0.1mm/min until the specimen failed. The force applied and corresponding stroke displacement was automatically recorded during the entire test.

Determination of Stress Intensity Factors by FE Analysis

Four 3-dimensional finite element models representing the respective beam groups were generated using PATRAN 8.5 [10]. Generally, 20-node second-order quadratic brick elements were used in the model. Around the crack front, however, triangular prismatic elements [11] formed by collapsing one face of corresponding brick elements, and with the four mid-side nodes moved to their quarter points, were employed. Figure 5 shows the entire assembly for a beam group, which consisted of 5944 elements and 27019 nodes.

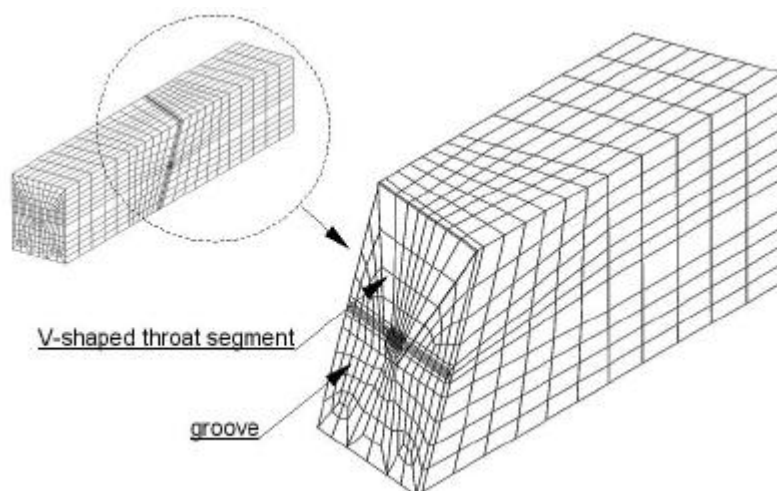


Figure 5: Finite element mesh for beam group A

The numerical analyses were carried out by ABAQUS 5.8 [12] and the stress intensity factors, K_I , K_{II} and K_{III} , for each layer of elements across the throat, and in each case of unit loading, were obtained from the corresponding nodal displacements of the crack face. The stress intensity factors along the crack front were thereby obtained. Figure 6 shows the distributions of K_I , K_{II} and K_{III} for one of the beam groups.

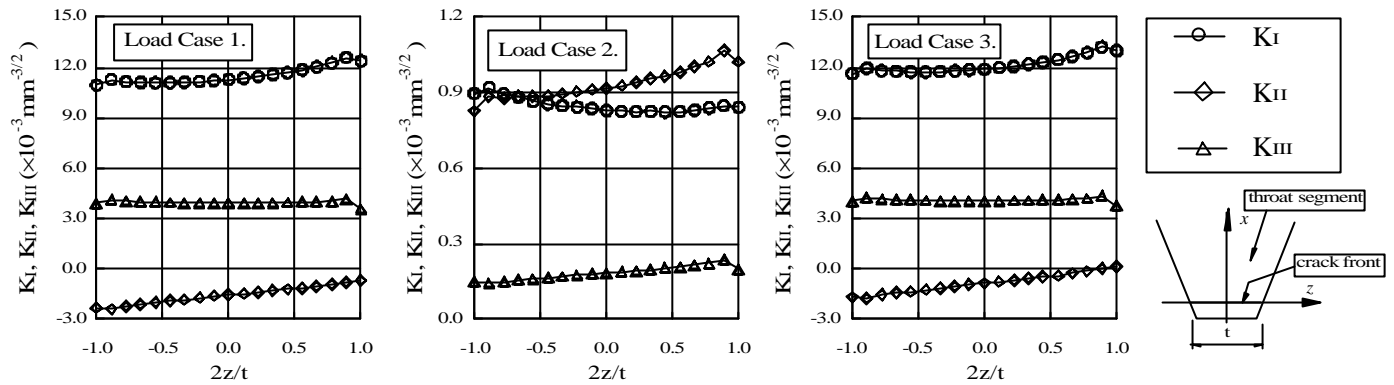


Figure 6: Distributions of stress intensity factors across crack front of beam group

RESULTS AND CONCLUSIONS

For each of the beam groups, three specimens have been tested under each category of loading case. Accordingly, thirty-six beam specimens were tested in all.

In all cases, the load was found to rise with stroke displacement initially. Crack extension started when the load reached its critical value of F_C . As illustrated in Figure 7, the values of F_C were significantly greater under four-point shear loading than under four- or three-point bending. In the cases of three- and four-point bending, the load decreased gradually after F_C , until failure occurred in the specimen. This implies that additional energy was required to maintain crack extension. However, in the case of four-point shear, the peak load dropped suddenly, and the specimen was subjected to sudden failure.

The cracks were found to extend along the grooved segment initially, and after a certain stage, deviated from the throat segment to extend vertically upwards (Figure 8). The reason of such a deviation was that when the crack approached the top face of the specimen, the length of the crack front increased. Thus, by a certain stage, the effect of grooving would not be sufficient to guide the crack along the grooved segment and the crack would extend along the more critical direction, which was upwards.

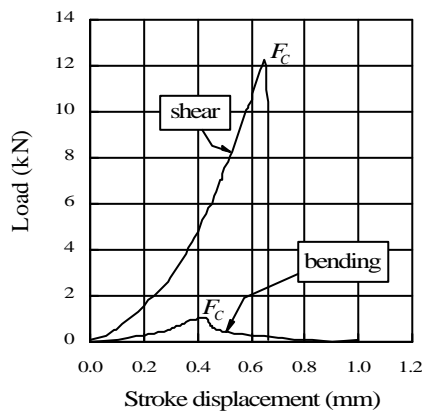


Figure 7: Typical load-stroke displacement curves for bending and shear loading



Figure 8: Failure of specimen

The fracture toughness in pure modes I, II and III had been evaluated in earlier tests on the same material as being 0.468MPa m, 0.759MPa m and 1.12MPa m respectively. For each of the present mixed mode fracture cases, $K_{I\theta}$, $K_{II\theta}$ and $K_{III\theta}$ were obtained via

$$K_{I\theta} = K_I \times F_C, \quad (11)$$

$$K_{II\theta} = K_{II} \times F_C \quad (12)$$

and

$$K_{III\theta} = K_{III} \times F_C, \quad (13)$$

where K_I , K_{II} and K_{III} were the stress intensity factors obtained from numerical analyses, and F_C the critical load measured in corresponding tests. The test results are depicted in the plot shown in Figure 9. The figure also shows the unified fracture envelope defined by Eqn. 10 superimposed on the results of the fracture tests. Accordingly, the agreement between prediction and experimental results was within 10%.

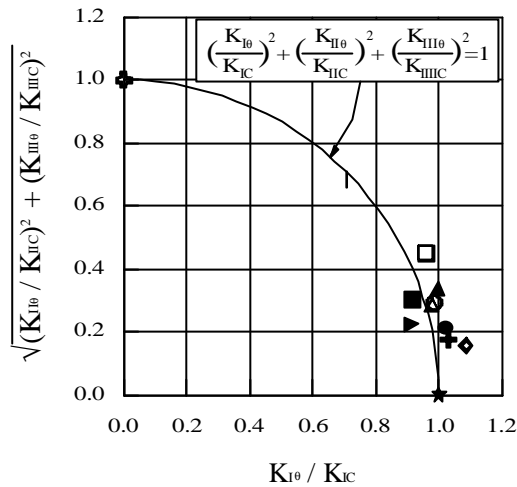


Figure 9: Comparison of unified fracture envelope with test results (different symbols for various loading and specimen configurations)

In view of the preceding findings, the following conclusion may be drawn: -

A generalized mixed mode I, II and III fracture criterion has been proposed as an extension of the *unified model*, based on the notion of a simple conversion of pure mode to mixed mode loading energy, in direct proportion to their respective fracture energies. A corresponding test method has been proposed to characterize the fracture of material subjected to mixed mode I, II and III loading. On the basis of the proposed fracture criterion and pure mode fracture toughness obtained from earlier tests, the experimental results show reasonably good agreement with the extended *unified model* prediction.

REFERENCES

- 1 Erdogan, F. and Sih, G.C. (1963) *J. Bas. Eng.*, *ASME Trans.* 85, 519.
- 2 Sih, G.C. (1974) *Int. J. Fract.* 10, 305.
- 3 Chen, X.M., Jiao, G.Q. and Cui, Z.Y. (1986) *Eng. Fract. Mech.* 24, 127.
- 4 Qian, J. and Fatemi, A. (1996) *Eng. Fract. Mech.* 55, 969.
- 5 Richard, H.A. and Kuna, M. (1990) *Eng. Fract. Mech.* 5, 949.
- 6 Hyde, T.H. and Aksogan, O. (1994) *J. Strain Analysis*, 29, 1.
- 7 Lo, K.W., Tamilselvan, T., Chua, K.H. and Zhao, M.M. (1996) *Eng. Fract. Mech.* 54, 189.
- 8 Lo, K. W., Zhong, K. and Tamilselvan, T. Invited keynote lecture presented at MicroMaterials Conference *MicroMat 2000*, Berlin, April 17-19, 2000.
- 9 British Standard Institution, BS 1881: Part 116, "Methods for Determination of Compressive Strength of Concrete Cubes", 1983.

- 10 The MacNeal-Schwendler Corporation. (1999) *PATRAN Version 8.5*. USA.
- 11 Barsoum, R.S. (1976) *Int. J. Numerical Method in Eng.* 10, 35.
- 12 Hibbit, Karlsson and Sorensen, Inc. (1998) *ABAQUS Version 5.8*. USA.